

Quantitative Analysis of ^{18}F -PF-06684511, a Novel PET Radioligand for Selective β -secretase 1 Imaging, in Non-human Primate Brain

Akihiro Takano¹, Laigao Chen², Sangram Nag¹, Michael A. Brodney², Ryosuke Arakawa¹, Cheng Chang³, Nahid Amini¹, Shawn D. Doran³, Jason K. Dutra³, Timothy J. McCarthy², Charles E. Nolan², Brian T. O'Neill³, Anabella Villalobos³, Lei Zhang², Christer Halldin¹

1 Department of Clinical Neuroscience, Centre for Psychiatry Research, Karolinska Institutet and Stockholm County Council, Stockholm SWEDEN

2 Worldwide Research & Development, Pfizer Inc., Cambridge, MA, USA

3 Worldwide Research & Development, Pfizer Inc., Groton, CT, USA

Corresponding author: Akihiro Takano, MD, PhD

Tel: +46 8 517 750 15

E-mail: Akihiro.Takano@ki.se

key words: BACE, PET, Alzheimer disease, non-human primate

Running title: Brain BACE1 in nonhuman primates

ABSTRACT

Beta-secretase 1 (BACE1) is a key enzyme in the generation of beta-amyloid, which is accumulated in the brain of Alzheimer's disease (AD) patients. PF-06684511 was identified as a candidate PET ligand for imaging BACE1 in the brain, and showed high specific binding in an initial assessment in a non-human primate (NHP) PET study utilizing ^{18}F -PF-06684511. In this effort, we aimed to quantitatively evaluate the regional brain distribution of ^{18}F -PF-06684511 in NHPs under baseline and blocking conditions as well as assess the target occupancy of BACE1 inhibitors. In addition, NHP whole body PET measurements were performed to estimate the effective radiation dose. **Methods:** Initial brain PET measurements were performed at baseline and after oral administration of 5 mg/kg of LY2886721, a BACE1 inhibitor, in two cynomolgus monkeys. Kinetic analysis was performed with the radiometabolite-corrected plasma input function. In addition, a wide dose range of another BACE1 inhibitor, PF-06663195, was examined to investigate the relationship between the brain target occupancy and plasma concentration of the drug. Finally, the effective radiation dose of ^{18}F -PF-06684511 was estimated based on the whole body PET measurements in NHPs. **Results:** Radiolabeling was accomplished successfully with an incorporation radiochemical yield of 4-12% (decay corrected) from fluorine-18 ion. The radiochemical purity was greater than 99%. The whole brain uptake of ^{18}F -PF-06684511 reached peak (approximately 220% SUV) at approximately 20 minutes and decreased

thereafter (approximately 100% SUV at 180 minutes). Two-tissue compartment model described the time activity curves well. Pre-treatment with LY2886721 reduced the total distribution volume of ^{18}F -PF-06684511 by 48 – 80% depending on the brain regions, confirming its *in vivo* specificity. BACE1 occupancy of PF-06663195, estimated using Lassen occupancy plot, showed a dose-dependent increase. The effective dose of ^{18}F -PF-06684511 was 0.043 mSv/MBq for humans. **Conclusion:** ^{18}F -PF-06684511 is the first successful PET radioligand for BACE1 brain imaging that demonstrates favorable *in vivo* binding and brain kinetics in NHPs. (306/350 words)

Keywords: BACE1; brain; non-human primate; occupancy; PET; radiation dose

INTRODUCTION

Alzheimer's disease (AD) is the most common dementing disease in the elderly, characterized by extracellular accumulation of toxic beta-amyloid peptide ($A\beta$) and intraneuronal neurofibrillary tau tangles in the brain (1). $A\beta$ is produced by sequential β - and γ - secretase-mediated cleavage of the amyloid precursor protein (APP). β -secretase 1 (BACE1) is thought to be a key enzyme for $A\beta$ accumulation (2). In postmortem studies, mRNA and protein levels of BACE1 were reported to be increased in AD patients in comparison to normal controls (3-5). Recent amyloid PET imaging studies indicate that amyloid deposit starts 10 to 20 years before the onset of the disease, which suggests that $A\beta$ accumulation in the brain plays an important role in early stage of AD pathogenesis (6). Because BACE1-mediated cleavage of APP is one of the key processes to $A\beta$ accumulation, inhibition of BACE1 is expected to have therapeutic potential for treating AD. In APP transgenic mice, BACE1 inhibitors have been shown to significantly reduce $A\beta$ accumulation (7-10). In recent years, several BACE1 inhibitors have been investigated in clinical trials (11,12). Measurement of $A\beta$ concentration in cerebrospinal fluid and amyloid imaging have helped to prove the mechanism of action of the drugs. PET radioligands specifically binding to BACE1 may help the evaluation of the target engagement and the dose selection in clinical trials of BACE1 inhibitors, by directly measuring *in vivo* target occupancy. In addition, BACE1 expression levels in AD patients measured by a BACE1 selective PET radioligand may

potentially be applied to select the appropriate disease sub-population for clinical assessment of BACE1 inhibitors.

PF-06684511 has been identified and evaluated as a novel candidate PET ligand that binds to the BACE1 target ($IC_{50}= 0.7$ nM) (13). Upon radiolabeling with fluorine-18, it demonstrated favorable brain uptake and high binding specificity in non-human primates (NHPs) with PET imaging, suggesting it is a promising PET ligand for imaging BACE1 (13). In this research, three studies were performed as follows. First, we quantitatively evaluated the regional brain distribution of ^{18}F -PF-06684511 in NHPs under baseline and blocking conditions with a BACE1 inhibitor, LY2886721 (14). Second, a wide dose range of another BACE1 inhibitor, PF-06663195 (15), was examined to investigate the relationship between the target occupancy and plasma concentration of the drug. Lastly, the effective radiation dose of ^{18}F -PF-06684511 was estimated based on the NHP whole body PET measurements.

MATERIALS AND METHODS

Radioligand Synthesis

^{18}F -PF-06684511 was synthesized as reported previously (13).

Subjects

A total of 7 cynomolgus monkeys (2 females, 5 males) (body weight: 3725g to 9700g) were used in this research. Two NHPs [one female (NHP1), one male (NHP2)] were used in the baseline/blocking study. Four NHPs [two females (NHP1 and 3), two males (NHP4 and 5)] were used in the target occupancy study, with one female NHP (NHP1) used in both studies. Two male NHPs (NHP6 and 7) were used in the whole body dosimetry study.

The NHPs were housed in the Astrid Fagraeus Laboratory of the Swedish Institute for Infectious Disease Control (AFL), Solna, Sweden. All studies were approved by the Animal Ethics Committee of the Swedish Animal Welfare Agency (N185/14) and performed according to “Guidelines for planning, conducting and documenting experimental research” (Dnr 4820/06-600) of Karolinska Institutet.

Brain PET System

Brain PET measurements were conducted using a High Resolution Research Tomograph (Siemens Molecular Imaging). List-mode data were reconstructed using the ordinary Poisson-3D-ordered subset expectation maximization (OP-3D-OSEM) algorithm.

Drug Administration

LY2886721 was used in the baseline/blocking study. It was administered orally (via gavage) approximately 2 hours before PET scanning, at a dose of 5 mg/kg and a dosing volume of 2 mL/kg.

PF-06663195 was used in the target occupancy study. It was administered intravenously as a bolus (1 minute, volume: 0.1 mL/kg) followed by a constant (1.0 mL/hr/kg) infusion to the end of scan. The bolus injection was started approximately 10 minutes before PET scanning.

Four different doses (0.022 mg/kg + 0.005 mg/hr/kg, 0.089 mg/kg + 0.021 mg/hr/kg, 0.133 mg/kg + 0.032 mg/hr/kg and 0.266 mg/kg + 0.064 mg/hr/kg) of PF-06663195 were tested in this study. Based on our previous experience, intravenous (IV) bolus plus infusion dosing method typically result in more reliable and consistent plasma pharmacokinetic exposure than oral dosing in anesthetized NHPs. The IV infusion protocol was chosen based on predicted “IV bolus + infusion” pharmacokinetic profile using a Pfizer internal pharmacokinetic model, making use of data from a previously performed Pfizer pharmacokinetic study with bolus IV dosing of PF-06663195 in NHPs.

Brain PET Measurements

Anesthesia was induced by intramuscular injection of ketamine hydrochloride (approximately 10 mg/kg) and maintained by the administration of a mixture of isoflurane (1.5-2.0%), oxygen, and medical air with endotracheal intubation.

A transmission scan of 6 minutes using a single ^{137}Cs source was performed before the ^{18}F -PF-06684511 injection. List mode data were acquired continuously for 180 minutes (in the baseline/blocking study) and 123 minutes (in the target occupancy study) immediately after intravenous injection of the radioligand. Images were reconstructed with a series of 28 frames (1 minute \times 5, 3 minutes \times 5, 6 minutes \times 5, and 10 minutes \times 13) in the baseline/blocking study and with a series of 34 frames (20 sec \times 9, 1 minute \times 3, 3 minutes \times 5, and 6 minutes \times 17) in the target occupancy study. Each PET measurement for the same NHP was separated by at least 5 weeks. In the baseline/blocking study, one baseline and one blocking PET measurements were performed for each NHP. In the target occupancy study, one baseline and two blocking PET measurements were performed per NHP, corresponding to intravenous administration of two different doses of PF-06663195.

Arterial Blood Sampling

Arterial blood sampling system (ABSS) (Allogg AB) at a speed of 3 mL/minute was used to measure the continuous radioactivity in the blood for the first 3 minutes. The dispersion correction was made for the measured radioactivity. Thereafter blood sampling (1-3mL per sample) was performed manually for the measurement of metabolism and radioactivity at 4, 10, 20, 30, 45, 60, 90, 120 minutes (150 and 180 minutes in baseline/blocking study only).

Radiometabolite Analysis

A reversed-phase radio-high-performance liquid chromatography (HPLC) method was used to determine the amount of unchanged ¹⁸F-PF-06684511 and its radiometabolites in NHP plasma.

Protein Binding

The free fraction (f_p) of ¹⁸F-PF-06684511 in plasma was estimated using an ultrafiltration method (16).

Measurement of Plasma Concentration of LY2886721 and PF-06663195

Under the drug pre-treatment condition, venous blood samples (1 mL each) were taken at -125 minutes, -60 minutes, -1 minute, 60 minutes, 120 minutes and 180 minutes for LY2886721, and -13 minutes, -1 minute, 30 minutes, 60 minutes, 90 minutes, and 120 minutes for PF-06663195 when the time of the radioligand injection was time 0. Plasma concentration of

LY2886721 and PF-06663195 were measured at a pharmacokinetic analysis lab (Unilabs York Bioanalytical Solutions).

MRI Measurements

T1-weighted magnetic resonance images (MRIs) of the individual NHP brains had been obtained using a 1.5T General Electrics Signa (GE, Milwaukee, WI, USA) system. The MR sequence was a 3D spoiled gradient recalled protocol with the following settings: repetition time, 21 ms; flip angle, 35°; field of view, 12.8 cm; matrix, 256×256×128; 128×1.0 mm slices; and number of excitations, 2.

Brain Image Analysis

The image data including kinetic model analysis were analyzed using PMOD version 3.4 (PMOD Technologies LLC, Zurich, Switzerland). The volumes of interest (VOIs) were delineated manually on the MRI images of each NHP for the whole brain, and 13 brain regions: cerebellum, anterior cingulate cortex, frontal cortex, temporal cortex, caudate, putamen, thalamus, occipital cortex, parietal cortex, amygdala, hippocampus, insular cortex and ventral striatum areas. The summed PET images of all frames were co-registered to the MRI of the same

NHP (Supplemental Fig. 1). By applying the co-registration parameters to the dynamic PET data, the time-activity curves (TACs) of brain regions were generated for each PET measurement.

Kinetic Model Analysis

One-tissue compartment model (1TC) and two-tissue compartment model (2TC) were evaluated with the radiometabolite-corrected plasma radioactivity as the input function. Fractional blood volume was set to 5% in all regions. As the main outcome measure, the total distribution volume (V_T) defined as $K1/k2$ by 1TC and $K1/k2 \times (1+k3/k4)$ by 2TC was calculated.

The goodness of fit was assessed using Akaike information criteria (AIC).

Time stability of V_T was evaluated by truncating the PET data frame by frame.

Graphical Analysis

Logan graphical plot was used to estimate V_T (17) for the baseline/blocking study. T^* was determined based on the model function in PMOD software where the earliest sample time point of t^* was searched so that the deviation between the regression and all measurements is less than 10%. T^* was 4-20min in the baseline/blocking study.

To evaluate the correlation between V_T values estimated from 2TC and Logan graphical analysis, V_T values of 4 baseline PET measurements for the occupancy study were also calculated.

Estimation of the Target Occupancy

As there was no expected reference region, the target occupancy was estimated by Lassen occupancy plot (18,19) using V_T calculated by 2TC. The thirteen brain regions were included in the plot.

Relationship between BACE1 Occupancy and PF-06663195

The average plasma concentration (C_{ave}) was determined by area under the curve using the “trapezoidal rule” during a 120-minute PET scan of PF-06663195. The relationship between C_{ave} and the BACE1 occupancy in the brain was estimated by an E_{max} model, which is a single binding site model, with the following equation: $Occupancy (\%) = C/(EC_{50}+C) \times E_{max}$, where C is the plasma concentration of PF-06663195, EC_{50} is the plasma concentration required to achieve 50% of the maximum occupancy, and E_{max} is the maximum occupancy. In this analysis, E_{max} was set as 100%. Similarly, ED_{50} for the total dose was estimated.

Whole Body PET System

Whole body PET measurements were conducted using a Siemens Biograph TruePoint TrueV PET/CT system (Siemens Medical Solutions).

Whole Body PET Measurements

Anesthesia was induced by intramuscular injection of ketamine hydrochloride (approximately 10 mg/kg) at AFL and maintained by intravenous infusion of ketamine (4 mg/kg/h) and xylazine (0.4 mg/kg/h) with a pump. Before the PET scan, a whole body low-dose CT scan was obtained for attenuation correction. After intravenous bolus injection of ^{18}F -PF-06684511, a whole-body PET scan was performed for approximately 180 minutes.

Image Analysis of the Whole Body PET

VOIs were drawn on high uptake organs such as the brain, lung, heart, kidney, spleen, pancreas, liver, gall bladder, stomach, urinary bladder, small intestine, bone (lumbar vertebrae), and esophagus (only for one NHP) with the help of the CT images for anatomic landmarks.

Estimates of the absorbed radiation dose in humans were calculated with OLINDA/EXM 1.1 (Organ Level Internal Dose Assessment Code) software, using the adult male (70 kg) reference model (20).

RESULTS

Radioligand Synthesis

¹⁸F-PF-06684511 was successfully radiosynthesized within 80-95 minutes from the end of beam. Radiochemical purity was >99% and radiochemical yield was 4-12%. ¹⁸F-PF-06684511 was stable for two hours after the end of synthesis.

PET Data in the Baseline/blocking Study

The mean injected radioactivity (n=4) of ¹⁸F-PF-06684511 was 149±22 MBq (range 117–168 MBq). The mean molar activity at the time of injection was 103±49 GBq/μmol (range 73–175 GBq/μmol), and the mean injected mass was 0.7±0.3 μg (range 0.3–1.0 μg). The summed PET images at the baseline and under drug treatment are shown in Fig. 1. The brain uptake decreased after LY2886721 (5 mg/kg, PO) administration. TACs of the whole brain reached peak (approximately 220% SUV on average) at approximately 20 minutes and thereafter decreased (approximately 100% SUV at 180 minutes on average) at baseline, and the time at the peak became earlier at the pretreatment condition (Supplemental Fig. 2). Regional TACs of NHP 1 are shown in Fig. 2. The uptake was relatively higher in subcortical regions than in the cortical regions. The washout from the peak in the cerebellum was faster than that in other regions. The uptake decreased in all brain regions after the administration of LY2886721. Average TACs at

baseline of 180-minute PET data (n=2) and 120-minute PET data (n=4) were shown in Supplemental Fig. 3AB.

Radioligand in Plasma

Approximately 40% of ^{18}F -PF-06684511 remained to be unmetabolized in the plasma of NHP 1 at 90 minutes (Fig. 3). There were no radiometabolites showing higher lipophilicity than ^{18}F -PF-06684511 (Supplemental Fig. 4). The average fraction of the unchanged radioligand for the baseline/blocking study and the occupancy study is shown in Supplemental Fig. 5. Plasma free fraction was 23.4% and 18.8% at the baseline and 22.4% and 29.2% at the pretreatment in NHP 1 and 2, respectively.

Kinetic Analysis, and Target Occupancy of LY2886721

In most regions, both 1TC and 2TC described the TACs well while 2TC described better in some regions such as the hippocampus (Fig. 4). When the first two NHPs' baseline data were combined, 18 out of 26 brain regions showed better fit with 2TC for AIC. Estimated kinetic parameters and V_T are shown in Supplemental Table 1 for 1TC and Supplemental Table 2 for 2TC. V_T values were correlated well between 1TC and 2TC ($R^2 > 0.99$). Individual V_T values estimated by 2TC were shown in Supplemental Fig. 6. V_T decreased in all brain regions after

administration of LY2886721 (48-80%). Lassen occupancy plots are shown in Supplemental Fig.

7. The estimated occupancy after LY2886721 pretreatment was 91.6% and 92.1%. V_{ND} was estimated to be 2.7 and 3.1 for NHP 1 and 2, respectively.

Time Stability of Estimated V_T

The percent change of V_T from the V_T calculated using 180-minute data is shown in Supplemental Fig. 8. The 120-minute data showed less than 10% change in all investigated brain regions, and less than 5% in most brain regions.

Graphical Analysis

Examples of Logan graphical plots were shown in Supplemental Fig. 9. V_T values estimated by Logan graphical plots were shown in Supplemental Table 3. The correlation between V_T estimated by Logan graphical plot and 2TC was shown in Supplemental Fig. 10. When a linear regression without an intercept was made, the regression equation was expressed as $y = 0.9376x$ (R^2 was 0.99). V_T values estimated with Logan plot were negatively biased by approximately 6%, compared with those estimated with 2TC.

PET Data in the Target Occupancy Study

The mean injected radioactivity (n=12) of ^{18}F -PF-06684511 was 156 ± 6 MBq (range 143–165 MBq). The mean molar activity at the time of injection was 69 ± 32 GBq/ μmol (range 32–133 GBq/ μmol), and the mean injected mass was 1.2 ± 0.5 μg (range 0.5–2.1 μg). The uptake of ^{18}F -PF-06684511 decreased in all brain regions with administration of PF-06663195. The target occupancies estimated using Lassen occupancy plots with V_T were 39.5% – 98.1% (examples in Supplemental Fig. 11). Estimated V_{ND} was 3.72 ± 0.87 (2.70-5.24). The time courses of the plasma concentration of PF-06663195 were shown in Supplemental Fig. 12. Exposure-occupancy curve was well fitted with an E_{max} model. EC_{50} was estimated to be 3.75 ng/mL (Fig. 5). ED_{50} was estimated to be 0.049 mg/kg (Supplemental Fig. 13).

Whole Body PET

The injected radioactivity of ^{18}F -PF-06684511 was 219 and 200 MBq, respectively. The molar activity at the time of injection was 30 and 32 GBq/ μmol , and the injected mass was 3.2 and 2.7 μg , respectively. The highest average uptake (%ID) was found in the stomach (approximately 34% at 175 minutes), followed by liver (approximately 18% at around 11 minutes) (Fig. 6). The radioligand was partly excreted via the bile and gastrointestinal tract, and partly excreted through the urinary tract (Fig. 6; Supplemental Fig. 14). The numbers of

disintegrations in the source organs are shown in Supplemental Table 4. The largest absorbed dose was found in the stomach wall (0.22 mSv/MBq) (Supplemental Table 5). The calculated human whole body effective dose was about 0.043 mSv/MBq (Supplemental Table 5).

DISCUSSION

A novel PET radioligand for BACE1, ^{18}F -PF-06684511, was evaluated in NHPs and showed favorable characteristics as a PET radioligand, with high brain uptake and high specific binding in the present study. Development of PET radioligands for BACE1 was attempted previously. ^{11}C -Me-NCFB was developed, but no evaluation using PET imaging was performed (21). Further study using the radioligand has not been reported so far. ^{11}C -BSI-IV was also reported to be a potential PET radioligand for BACE1, but low uptake in rodents and low degree of specific binding lead to limited use (22).

In this study, V_T estimated using 2TC showed regional differences, with cerebellum being the lowest (23), and this regionality corresponds to the distribution of BACE1 in the brain. No reference region was identified due to the fact that the estimated V_T values in all brain regions evaluated including cerebellum decreased after the administration of a BACE1 inhibitor. As an exploratory evaluation, the white matter was also investigated as a potential reference region, but the uptake in the white matter decreased after the administration of a BACE1 inhibitor

(Supplemental Fig. 15AB). The estimated V_{ND} from Lassen plot was approximately three while the V_T values were ranging from six to eighteen. The ratios of specific to nonspecific binding were in the range of one to six. This meant that about 50 to 86% of V_T was specific depending on brain regions.

The time stability of V_T values showed that most of the investigated brain regions had less than 5% change from 180 minutes to 120 minutes. It was considered to be sufficient to perform 120-minute PET measurements for ^{18}F -PF-06684511 in NHPs.

In the radio-HPLC analysis, there were no radiometabolites showing higher lipophilicity than ^{18}F -PF-06684511. Although the results could not completely exclude the possibility of brain permeable radiometabolites, the impact of radiometabolites on the quantitative analysis was thought to be low as the PET data were well described by one- and two-tissue compartment model using the metabolite-corrected plasma as the input function. The goodness of fit was assessed for the blocking data of the first two NHPs with LY2886721, by which the binding of ^{18}F -PF-06684511 was almost fully blocked. AIC showed better fit with 1TC than 2TC in 21 out of 26 TACs. This may indicate that it is less likely there were radiometabolites entering into the brain, which would contribute to the second tissue compartment. The time stability of V_T in the blocking study was shown in Supplemental Fig. 16. It also supports the hypothesis that there was minimal contribution of radiometabolites in the

quantification of the radioligand uptake in the brain, since the truncation of the dynamic scan data did not lead to significant bias in any brain regions.

BACE1 inhibition has been one of the active targets for drug development for AD (24,25). Clinical development of several BACE1 inhibitors such as E2609 (NCT03036280 and NCT02956486), LY3202626 (NCT03367403) and CNP520 (NCT03131453 and NCT02565511) are still active while clinical trials of some other BACE inhibitors such as MK-8931 (NCT01739348 and NCT01953601) and lanabecestat (NCT02245737) were terminated due to insufficient efficacy. So far the clinical trials of BACE1 inhibitors have not shown promising results as initially expected (24,25). Timing of drug administration in the disease progress, patient selection and target engagement of the drugs may be potential factors contributing to the failure (24,25). BACE1 was reported to regulate neurogenesis in early developmental stages (26). A recent report showed that BACE1 regulates adult hippocampal neurogenesis, and that complete inhibition of BACE1 activity dysregulates adult hippocampal neurogenesis but partial inhibition would not impact it (27). Therefore partial inhibition of BACE1 activity was proposed as a more suitable therapeutic approach. The balance between the A β depletion and adult hippocampal neurogenesis may be an important factor to improve the development strategy of BACE1 inhibitors. In this study, ¹⁸F-PF-06684511 showed high dynamic range in quantifying BACE1 binding as demonstrated by dose dependent occupancy with a BACE1 inhibitor, which allows

detection of small changes in BACE1 availability under disease or partial blockade conditions.

Potential application of ^{18}F -PF-06684511 PET in clinical trials of BACE1 inhibitors may include stratifying AD patients by measuring the BACE1 level in the brain, confirming the target engagement of the drugs, and fine-tuning the doses by measuring the *in vivo* occupancy.

Two BACE1 inhibitors, LY2886721 and PF-06663195, used to test the specific binding of ^{18}F -PF-06684511 to BACE1 in this study, share a fluorophenyl-pyrazine/pyridine-carboxamide substructure. It would be worth examining whether BACE1 inhibitors with different chemotypes compete with ^{18}F -PF-06684511 for binding sites in BACE1, as it would clarify the usefulness of ^{18}F -PF-06684511 in measurement of target engagement in general.

The whole body radiation dosimetry study showed a relatively high accumulation in the stomach. In NHP7, even esophagus was visualized in the late phase (Fig. 6). High uptake in the stomach could lead to relatively high effective doses compared with other F-18 radioligands (28). Some of the excretion from the liver to bile ducts and lower gastrointestinal tract appeared flow backward to the stomach and esophagus. The backflow may occur partially because the NHPs were lying down in the same position during the PET measurement under anesthesia with intravenous ketamine and xylazine. The stomach uptake is likely to be reduced in the human subjects because they are awake and movement of the whole body is possible during break times.

CONCLUSION

¹⁸F-PF-06684511 demonstrated favorable characteristics as a PET radioligand for BACE1 in NHPs with high brain uptake and clear blocking effects by BACE1 inhibitors. Further evaluation of this radioligand in humans is warranted.

ACKNOWLEDGEMENTS

Authors thank all the members of the Karolinska PET group for their assistance in PET experiments, including special thanks to Kia Hultberg-Lundberg and Jonas Ahlgren for excellent technical assistance. Authors would like to thank Dr. Michael Stabin (Vanderbilt University) for helping in calculation of the absorbed radiation dose.

Compliance with Ethical Standards

Disclosure of potential conflicts of interest

This work was sponsored by Pfizer Inc. Laigao Chen, Michael A. Brodney, Cheng Chang, Shawn D. Doran, Jason K. Dutra, Timothy J. McCarthy, Charles E. Nolan, Brian T. O'Neill, Anabella Villalobos, and Lei Zhang were employees of Pfizer Inc. when the study was conducted. No other potential conflicts of interest relevant to this article exist.

Statement on the welfare of animals

All studies were approved by the Animal Ethics Committee of the Swedish Animal Welfare Agency (N185/14) and performed according to “Guidelines for planning, conducting and documenting experimental research” (Dnr 4820/06-600) of Karolinska Institutet.

REFERENCES

1. Ballard C, Gauthier S, Corbett A, Brayne C, Aarsland D, Jones E. Alzheimer's disease. *Lancet*. 2011;377:1019-1031.
2. Yan R, Vassar R. Targeting the β secretase BACE1 for Alzheimer's disease therapy. *Lancet Neurol*. 2014;13:319-329.
3. Fukumoto H, Cheung BS, Hyman BT, Irizarry MC. Beta-secretase protein and activity are increased in the neocortex in Alzheimer disease. *Arch Neurol*. 2002;59:1381-1389.
4. Yang LB, Lindholm K, Yan R, et al. Elevated beta-secretase expression and enzymatic activity detected in sporadic Alzheimer disease. *Nat Med*. 2003;9:3-4.
5. Li R, Lindholm K, Yang LB, et al. Amyloid beta peptide load is correlated with increased beta-secretase activity in sporadic Alzheimer's disease patients. *Proc Natl Acad Sci U S A*. 2004;101:3632-3637.
6. Rodriguez-Vieitez E, Saint-Aubert L, Carter SF, et al. Diverging longitudinal changes in astrocytosis and amyloid PET in autosomal dominant Alzheimer's disease. *Brain*. 2016;139:922-936.
7. Eketjäll S, Janson J, Jeppsson F, et al. AZ-4217: a high potency BACE inhibitor displaying acute central efficacy in different in vivo models and reduced amyloid deposition in Tg2576 mice. *J Neurosci*. 2013;33:10075-10084.
8. Hussain I, Hawkins J, Harrison D, et al. Oral administration of a potent and selective non-peptidic BACE-1 inhibitor decreases beta-cleavage of amyloid precursor protein and amyloid-beta production in vivo. *J Neurochem*. 2007;100:802-809.

9. Neumann U, Rueeger H, Machauer R, et al. A novel BACE inhibitor NB-360 shows a superior pharmacological profile and robust reduction of amyloid- β and neuroinflammation in APP transgenic mice. *Mol Neurodegener.* 2015;10:44.
10. Sankaranarayanan S, Price EA, Wu G, et al. In vivo beta-secretase 1 inhibition leads to brain Abeta lowering and increased alpha-secretase processing of amyloid precursor protein without effect on neuregulin-1. *J Pharmacol Exp Ther.* 2008;324:957-969.
11. Vassar R. BACE1 inhibitor drugs in clinical trials for Alzheimer's disease. *Alzheimers Res Ther.* 2014;6:89.
12. Yan R. Stepping closer to treating Alzheimer's disease patients with BACE1 inhibitor drugs. *Transl Neurodegener.* 2016;5:13.
13. Zhang L, Chen L, Dutra JK, et al. Identification of a novel positron emission tomography (PET) ligand for imaging β -site amyloid precursor protein cleaving enzyme 1 (BACE-1) in brain. *J Med Chem.* 2018;61:3296-3308.
14. May PC, Willis BA, Lowe SL, et al. The potent BACE1 inhibitor LY2886721 elicits robust central A β pharmacodynamic responses in mice, dogs, and humans. *J Neurosci.* 2015;35:1199-1210.
15. Brodney MA, Beck EM, Butler CR, et al. Utilizing structures of CYP2D6 and BACE1 complexes to reduce risk of drug-drug interactions with a novel series of centrally efficacious BACE1 inhibitors. *J Med Chem.* 2015;58:3223-3252.
16. Amini N, Nakao R, Schou M, Halldin C. Determination of plasma protein binding of positron emission tomography radioligands by high-performance frontal analysis. *J Pharm Biomed Anal.* 2014; 98:140-143.

17. Logan J, Fowler JS, Volkow ND et al., Graphical analysis of reversible radioligand binding from time-activity measurements applied to [N-11C-methyl]-(-)-cocaine PET studies in human subjects. *J Cereb Blood Flow Metab.* 1990;10:740-747.
18. Cunningham VJ, Rabiner EA, Slifstein M, Laruelle M, Gunn RN. Measuring drug occupancy in the absence of a reference region: the Lassen plot re-visited. *J Cereb Blood Flow Metab.* 2010;30:46-50.
19. Lassen NA, Bartenstein PA, Lammertsma AA, et al. Benzodiazepine receptor quantification in vivo in humans using [¹¹C]flumazenil and PET: application of the steady-state principle. *J Cereb Blood Flow Metab.* 1995;15:152-165.
20. Stabin MG, Sparks RB, Crowe E. OLINDA/EXM: the second-generation personal computer software for internal dose assessment in nuclear medicine. *J Nucl Med.* 2005;46:1023-1027.
21. Kawai T, Kawashima H, Kuge Y, Saji H. Synthesis and evaluation of 11C-labeled naphthalene derivative as a novel non-peptidergic probe for the β -secretase (BACE1) imaging in Alzheimer's disease brain. *Nucl Med Biol.* 2013;40:705-709.
22. Nordeman P, Estrada S, Odell LR, et al. 11C-Labeling of a potent hydroxyethylamine BACE-1 inhibitor and evaluation in vitro and in vivo. *Nucl Med Biol.* 2014;41:536-543.
23. Shinohara M, Petersen RC, Dickson DW, Bu G. Brain regional correlation of amyloid- β with synapses and apolipoprotein E in non-demented individuals: potential mechanisms underlying regional vulnerability to amyloid- β accumulation. *Acta Neuropathol.* 2013;125:535-547.
24. Evin G. Future therapeutics in Alzheimer's disease: development status of BACE inhibitors. *BioDrugs.* 2016;30:173-194.
25. Coimbra JRM, Marques DFF, Baptista SJ, et al. Highlights in BACE1 inhibitors for Alzheimer's disease treatment. *Front Chem.* 2018;6:178.

26. Hu X, He W, Luo X, Tsubota KE, Yan R. BACE1 regulates hippocampal astrogenesis via the Jagged1-Notch pathway. *Cell Rep.* 2013;4:40-49.
27. Chatila ZK, Kim E, Berlé C et al. BACE1 regulates proliferation and neuronal differentiation of newborn cells in the adult hippocampus in mice. *eNeuro.* 2018;5:e0067.
28. Zanotti-Fregonara P, Lammertsma AA, Innis RB. Suggested pathway to assess radiation safety of ¹⁸F-labeled PET tracers for first-in-human studies. *Eur J Nucl Med Mol Imaging.* 2013;40:1781-1783.

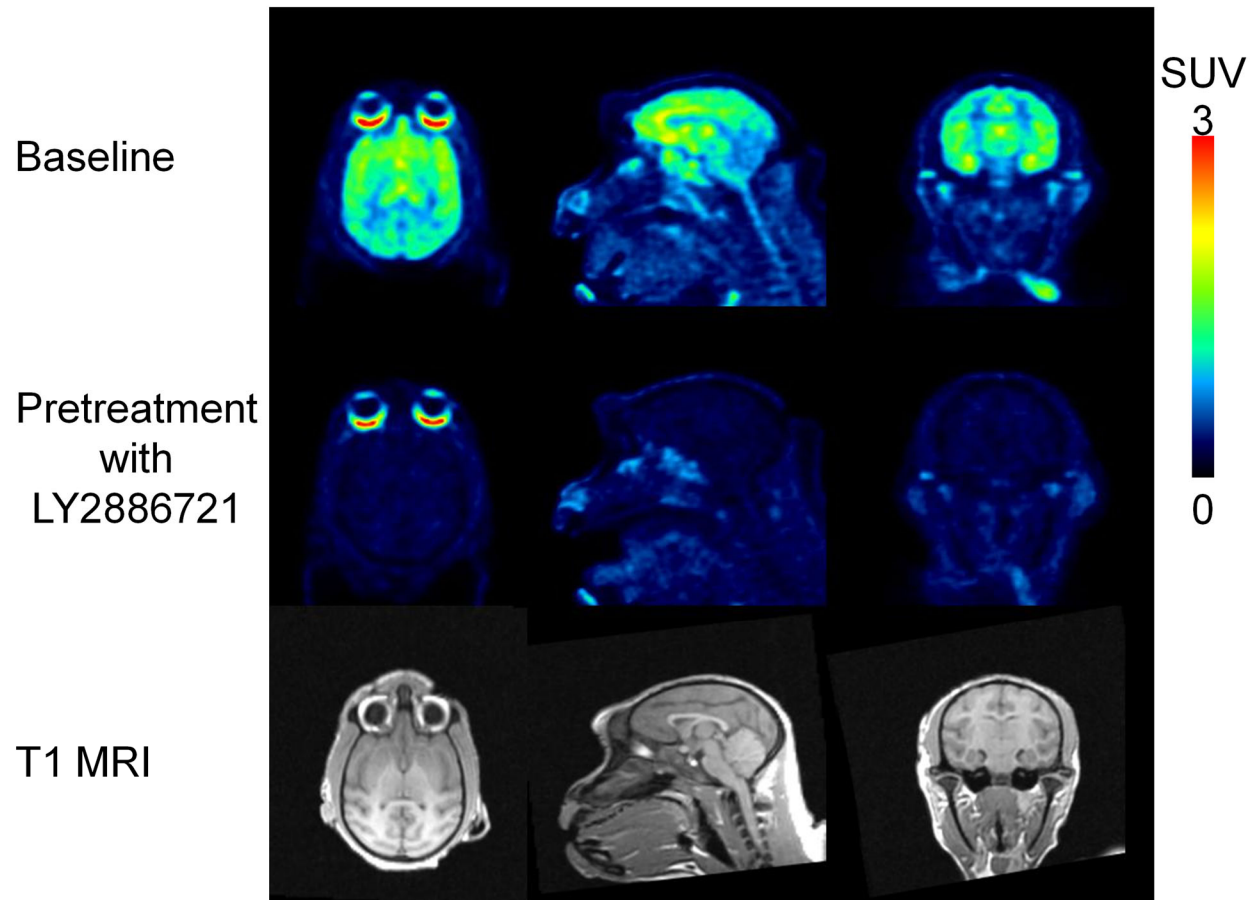


Fig. 1. PET images of ^{18}F -PF-06684511 summed from 90 minutes to 180 minutes at the baseline and under pretreatment of a BACE1 inhibitor, LY2886721 and corresponding MRI in NHP1.

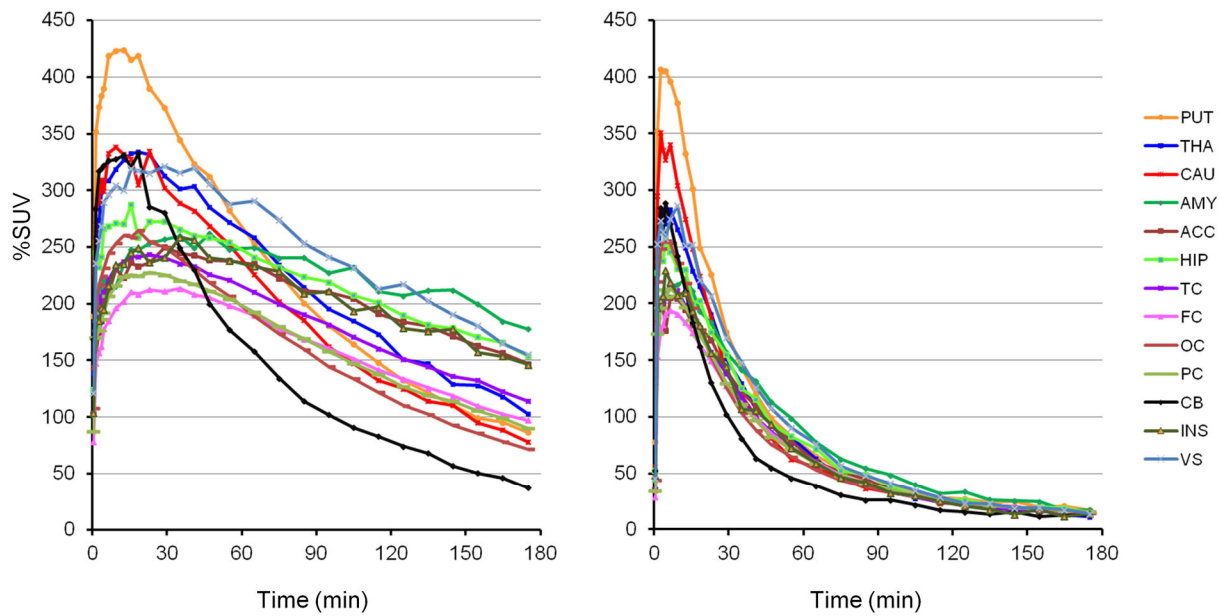


Fig. 2. Regional brain time activity curves of ^{18}F -PF-06684511 at the baseline (left) and pretreatment with LY2886721 (right) in NHP1.

PUT: putamen, THA: thalamus, CAU: caudate, AMY: amygdala, ACC: anterior cingulate cortex, HIP: hippocampus, TC: temporal cortex, FC: frontal cortex, OC; occipital cortex, PC: parietal cortex, CB: cerebellum, INS: insular cortex, VS: ventral striatum.

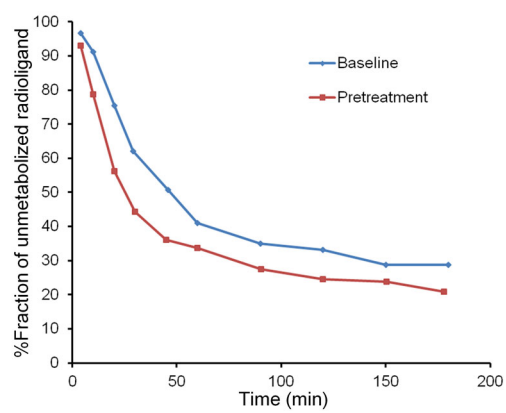


Fig. 3. Percent fraction of unmetabolized ^{18}F -PF-06684511 in the plasma in NHP 1.

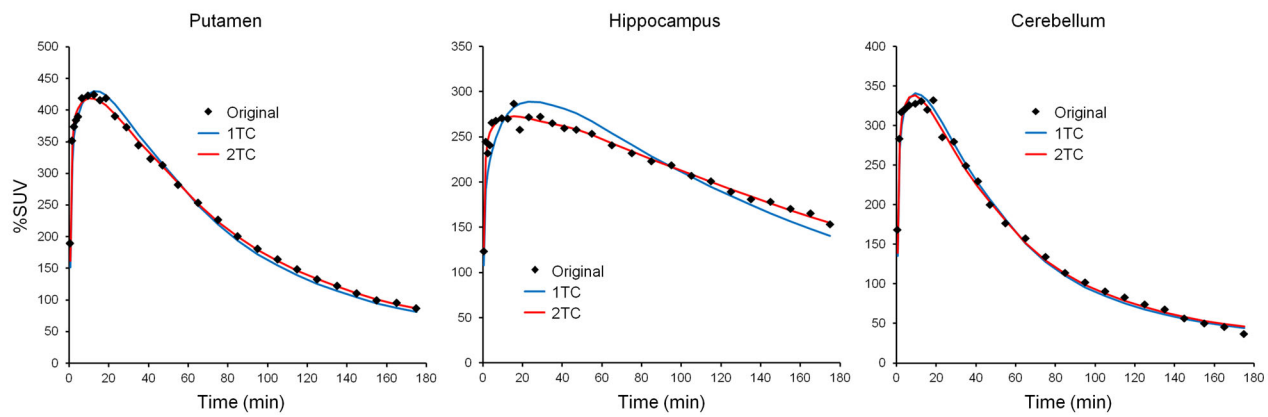


Fig. 4. Typical compartment model curve fitting of ^{18}F -PF-06684511. The data were from the baseline PET of NHP1.

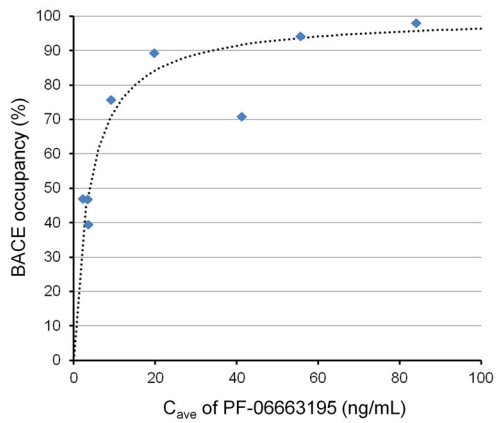


Fig. 5. The relationship between BACE1 occupancy and PF-06663195 average plasma concentration (C_{ave})

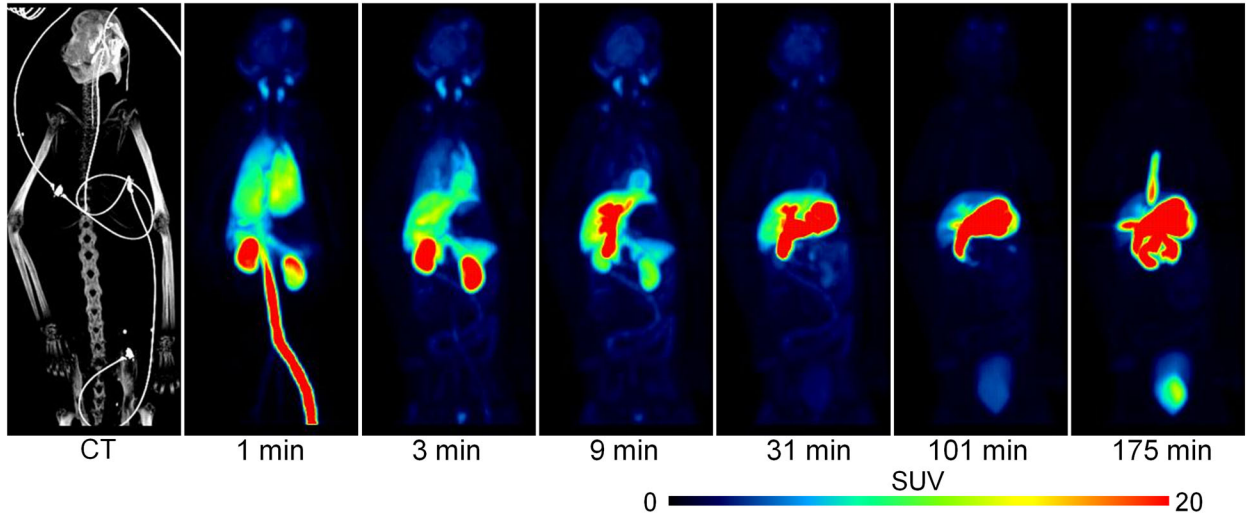


Fig. 6. Whole body PET images of ^{18}F -PF-06684511 in NHP7. Images are maximum intensity projection.